PHYSICAL REVIEW D **89,** 034008 (2014)

B_c exclusive decays to charmonium and a light meson at next-to-leading order accuracy

Cong-Feng Qiao,[1,*] Peng Sun,[2,3,†] Deshan Yang,[1,‡] and Rui-Lin Zhu[1,§]

[1]*Department of Physics, University of Chinese Academy of Sciences, YuQuan Road 19A, Beijing 100049, China*

[2]*Center for High-Energy Physics, Peking University, Beijing 100871, China*

[3]*Nuclear Science Division, LBNL, Berkeley, California 94720, USA*

(Received 2 December 2013; published 7 February 2014)

In this paper, we study the B_c-meson exclusive decays to S-wave charmonia and light pseudoscalar or vector mesons, i.e., π, K, ρ, and K^* at the next-to-leading order (NLO) in the QCD coupling. The nonfactorizable contribution is included, which is absent in traditional naive factorization. Numerical results show that NLO QCD corrections markedly enhance the branching ratio with a K factor of 1.75 for $B_c^{\pm} \to \eta_c \pi^{\pm}$ and 1.31 for $B_c^{\pm} \to J/\psi \pi^{\pm}$ using certain input parameters. And the theoretical uncertainties for their branching ratios are reduced compared with that of direct tree-level calculation. In order to investigate the asymptotic behavior, the analytic form is obtained in the heavy quark limit, i.e., $m_b \to \infty$. We note that annihilation topologies contribute trivia in this limit, and the corrections at leading order in $z = m_c/m_b$ expansion come from form factors and hard spectator interactions. At last, some related phenomenologies are also discussed.

DOI: 10.1103/PhysRevD.89.034008 PACS numbers: 12.38.Bx, 12.39.St, 13.20.He

I. INTRODUCTION

B_c and its excited states construct the unique meson family containing two different kinds of heavy flavor. The studies on the production and decay of B_c can shed light on the understanding of the strong interaction in such a unique system. In contrast to other bottom mesons embodying just one heavy flavor which can be produced remarkably through the e^+e^- and ep collisions, the cross section of B_c is suppressed owing to the associated production of two additional heavy quarks, c and $\bar{b}$ [1]. Thus, massive B_c events can only refer to the hadron colliders.

After the first discovery of B_c was reported by the CDF Collaboration at Tevatron in 1998 [2], there have been continuous measurements of its mass in different detectors via two different channels: $B_c^{\pm} \to J/\psi \ell^{\pm} v_{\ell}$ [3,4] and $B_c^{\pm} \to J/\psi \pi^{\pm}$ [5,6]. Especially for the latter exclusive two-body decay, it takes advantage of a large trigger efficiency. Using this channel, the LHCb Collaboration have measured the B_c mass with $6273.7 \pm 1.3(\text{stat}) \pm 1.6(\text{sys})$ MeV$/c^2$ recently [7]. However, the exact values of the branching ratios for $B_c^{\pm} \to J/\psi \ell^{\pm} v_{\ell}$ and $B_c^{\pm} \to J/\psi \pi^{\pm}$ have not been measured yet. And more channels should be involved to investigate the intrinsic properties of B_c. Up to now, the LHCb Collaboration have successfully observed more channels beyond the two kinds in question. And they have measured the new channels, $B_c^{+} \to J/\psi \pi^{+}\pi^{-}\pi^{+}$ [8], $B_c^{\pm} \to J/\psi K^{\pm}$ [9], $B_c^{\pm} \to \Psi(2S)\pi^{\pm}$ [10], and $B_c^{\pm} \to J/\psi D_s^{+}$ [11], for the first time. The study of the decay properties of B_c from a multitude of processes can help us to understand the quark flavor mixing and provide precision determination of the CKM matrix parameters. Furthermore, according to Refs. [12–14], the cross section of B_c is expected to $\sim$40 nb at the pp center-of-mass energy $\sqrt{s} = 14$ TeV. That means that around 10^{10} B_c mesons per year can be anticipated at the LHC. Thus, one should expect that a greater variety of decay channels of B_c will be measurable in the upcoming experiment.

Theoretically, the exclusive two-body decay of the B meson is studied within the frame of naive factorization [15], the pQCD method [16], and QCD factorization [17–20] in the heavy quark limit. Along with the technique for the QCD factorization for the exclusive hard processes, such as π electromagnetic form factors at the large momentum transfer and B-meson decays to two light mesons, many theorists believe that the QCD factorization for $B_c^{-} \to J/\psi \pi^{-}$ holds in the heavy quark limit generally. However, there are no complete or consistent predictions based at next-to-leading order (NLO) in α_s so far.

Since B_c^{-} contains two kinds of heavy quark, namely b and c quarks, the heavy quark limit may be realized in the nonrelativistic QCD (NRQCD) approach. Therein, one lets m_b, $m_c \to \infty$ and keeps the ratio $z \equiv m_c/m_b$ fixed. Then the decay amplitude of $B_c^{-} \to J/\psi(\eta_c)\pi^{-}$ is conjectured to be factorized:

$$\mathcal{A}(B_c^{-} \to J/\psi(\eta_c)\pi^{-}) \sim \Psi_{c\bar{c}}(0)\Psi_{b\bar{c}}(0) \times \int_0^1 dx T_H(x,\mu)\phi_{\pi}(x,\mu) + \mathcal{O}(1/m_b) + \mathcal{O}(v^2). \quad (1)$$

Here $\Psi_{c\bar{c}}(0)$ and $\Psi_{b\bar{c}}(0)$ denote the Schrödinger wave functions of $J/\psi(\eta_c)$ and B_c^{-}, respectively, at the origin.

*qiaocf@ucas.ac.cn
†sunp@pku.edu.cn
‡yangds@ucas.ac.cn
§zhuruilin09@mails.ucas.ac.cn

$T_H(x,\mu)$ is the perturbatively calculable hard kernel, and $\phi_\pi(x,\mu)$ is the pion's light-cone distribution amplitude (LCDA).

The rough arguments of the validity of the above factorization are twofold: (1) The energetic pion ejected from the heavy quark system cannot sense the surrounded soft and collinear gluons due to the "color transparency" at the leading order of heavy quark expansion; the hadronization of the collinear quark pair into a pion is totally described by the leading twist LCDA of the pion, as is the case in $B \to \pi\pi$. (2) The charm quark in B_c needs a large momentum transfer (typically $q^2 \sim m_b m_c \sim 6\ \mathrm{GeV}^2$) to speed up for catching another energetic charm quark from the $b \to c$ weak transition to form a quarkonium. This large momentum transfer guarantees the necessary condition for the implementation of the perturbative QCD in this process; i.e., the transition from B_c to $J/\psi(\eta_c)$ at the large recoil can be described by the hard-gluon exchange, and the hadronization is to be described by the nonrelativistic wave functions (at the origin) of B_c and $J/\psi(\eta_c)$, as is done in many NRQCD factorizations for the exclusive quarkonia processes.

In this paper, we will adopt the factorization formula [Eq. (1)] to calculate $B_c \to J/\psi(\eta_c)\pi$ at the next-to-leading order of strong coupling α_s. In our calculation, we find that all the low-energy divergences, including soft, collinear, and Coulomb divergences, are either canceled with each other (for the soft interactions) or separated with each other to be absorbed into the LCDA and the wave functions. Thus, our work can be treated as a proof for the factorization formula [Eq. (1)] at one-loop level.

The sections are organized as follows: In Sec. II, we present a brief overview of the effective weak Hamiltonian. In Sec. III, we present the detailed computation in the nonrelativistic factorization scheme, and we also deliver the asymptotic behavior in the limit $z = m_c/m_b \to 0$. In Sec. IV, we implement our results to make some phenomenological predictions for the branching ratios of various B_c two-body decays to an S-wave quarkonium and a light meson, and some detailed discussions are also performed. At last, we conclude in Sec. V.

II. THE THEORETICAL FRAME

In the Standard Model (SM), $B_c^- \to J/\psi\pi^-$ occurs through a W-mediated charge-current process. However, since $m_W \gg m_{b,c}$, Λ_{QCD}, a large logarithm arises in the higher-order strong-interaction corrections. Thus, the RG-improved perturbation theory must be resorted. In the community of B physics, this turns out to be the effective weak Hamiltonian method. The effective weak Hamiltonian governing $B_c^- \to J/\psi\pi^-$ is

$$\mathcal{H}_{\mathrm{eff}} = \frac{G_F}{\sqrt{2}} V_{ud}^* V_{cb} (C_1(\mu) Q_1(\mu) + C_2(\mu) Q_2(\mu)), \quad (2)$$

with G_F being the Fermi constants, V_{ud} and V_{cb} the Cabibbo-Kobayashi-Maskawa (CKM) matrix elements, $C_{1,2}(\mu)$ the perturbatively calculable Wilson coefficients, and $Q_{1,2}(\mu)$ the effective four-quark operators

$$Q_1 = \bar{d}_\alpha \gamma^\mu (1-\gamma_5) u_\alpha \bar{c}_\beta \gamma_\mu (1-\gamma_5) b_\beta, \quad (3a)$$

$$Q_2 = \bar{d}_\alpha \gamma^\mu (1-\gamma_5) u_\beta \bar{c}_\beta \gamma_\mu (1-\gamma_5) b_\alpha, \quad (3b)$$

where α, β are color indices and the summation conventions over repeated indices are understood. For the conveniences of our later calculations, we will adopt another operator basis, i.e.,

$$Q_0 = \bar{d}_\alpha \gamma^\mu (1-\gamma_5) u_\alpha \bar{c}_\beta \gamma_\mu (1-\gamma_5) b_\beta, \quad (4a)$$

$$Q_8 = \bar{d}_\alpha T^A_{\alpha\beta} \gamma^\mu (1-\gamma_5) u_\beta \bar{c}_\rho T^A_{\rho\lambda} \gamma_\mu (1-\gamma_5) b_\lambda, \quad (4b)$$

where T^A is the generator of the fundamental representation for $\mathrm{SU_C}(3)$. Applying the Fierz rearrangement relation

$$T^A_{\alpha\beta} T^A_{\rho\lambda} = -\frac{1}{6}\delta_{\alpha\beta}\delta_{\rho\lambda} + \frac{1}{2}\delta_{\alpha\lambda}\delta_{\rho\beta}, \quad (5)$$

we have immediately

$$Q_0 = Q_1, \qquad Q_8 = -\frac{1}{6} Q_1 + \frac{1}{2} Q_2. \quad (6)$$

Consequently, for the Wilson coefficients, we have

$$C_0 = C_1 + C_2/3, \qquad C_8 = 2C_2. \quad (7)$$

Then, the decay amplitude of $B_c^- \to J/\psi(\eta_c)\pi^-$ can be written as

$$\begin{aligned}\mathcal{A}(B_c^- \to J/\psi(\eta_c)\pi^-) &= \langle J/\psi(\eta_c)\pi^- | \mathcal{H}_{\mathrm{eff}} | B_c^- \rangle \\ &= \frac{G_F}{\sqrt{2}} V_{ud}^* V_{cb} (C_0(\mu)\langle Q_0(\mu)\rangle \\ &\quad + C_8(\mu)\langle Q_8(\mu)\rangle). \end{aligned} \quad (8)$$

III. THE NONRELATIVISTIC APPROACH

Systematically, the nonrelativistic QCD effective theory provides a rigorous factorization formalism for the annihilation and production of heavy quarkonia [21]. In this framework, the heavy quarkonium's production comes from two steps: a Fock state such as $|q\bar{q}\rangle$, $|q\bar{q}g\rangle$ produced at short distance by a large momentum transfer process, followed by it binding to quarkonium at long distance.

In the process of $B_c^- \to J/\psi(\eta_c)\pi^-$, all the nonperturbative blinding effects are attributed to three factors: the pion's decay constant and the Schrödinger wave functions of $J/\psi(\eta_c)$ and B_c at the origin. The hard kernel, meanwhile, can be calculated perturbatively.

A. Leading order (LO)

The possible quark-level topologies for $B_c \to J/\psi(\eta_c)\pi$ are portrayed in Fig. 1, where we assign momentum

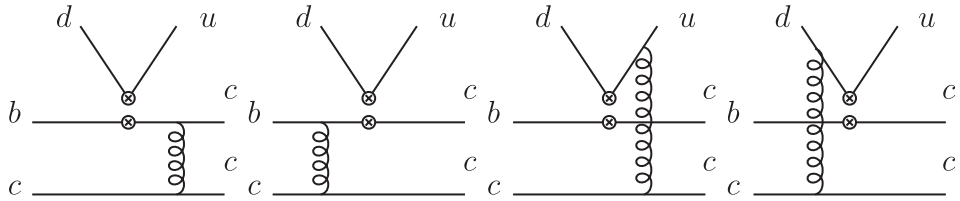

FIG. 1. The quark-level Feynman diagrams at leading order for $B_c \to J/\psi(\eta_c)\pi$. The 4-vertex "⊗⊗" denotes the insertion of a 4-fermion operator Q_i.

xP to the u quark and $(1-x)P$ to the d quark in the emitted pion. The leftmost two diagrams in Fig. 1 contribute to $\langle Q_0\rangle$, and the others contribute to $\langle Q_8\rangle$. Along with nonperturbative parameters: the pion's decay constant and the Schrödinger wave functions of $J/\psi(\eta_c)$ and B_c at the origin, and leaving the momentum fraction x unintegrated, we have the tree-level $\langle Q_i\rangle$:

$$\langle Q_0(\eta_c)\rangle_x = \frac{8\sqrt{2}\pi f_\pi \psi_{\eta_c}(0)\psi_{B_c}(0)\phi_\pi(x) C_A C_F \alpha_s \sqrt{m_b+m_c}(m_b+3m_c)(2m_b m_c+3m_b^2+3m_c^2)}{m_c^{3/2} N_c (m_b-m_c)^3},$$
$$\langle Q_8(\eta_c)\rangle_x = \frac{2\sqrt{2}\pi f_\pi \psi_{\eta_c}(0)\psi_{B_c}(0)\varphi_\pi(x) C_A C_F \alpha_s \sqrt{m_b+m_c}(m_b+3m_c)^2(xm_c-(x-1)m_b)}{m_c^{3/2} N_c^2 (m_c-m_b)((x-1)m_b+(3x-2)m_c)(xm_b+(3x-1)m_c)}, \tag{9}$$

where more detail on f_π, $\psi_{\eta_c}(0)$, $\psi_{B_c}(0)$, and the pion's LCDA $\phi_\pi(x,\mu)$ can be found in Appendix A. Note that the higher-twist contribution shall come from twist 4. Referring to J/ψ, we see that the corresponding matrix elements are

$$\langle Q_0(J/\psi)\rangle_x = -\frac{64\sqrt{2}\pi f_\pi \psi_{J/\psi}(0)\psi_{B_c}(0)\varphi_\pi(x) P_{B_c}\cdot\varepsilon_\Psi^* C_A C_F \alpha_s (m_b+m_c)^{5/2}}{m_c^{1/2} N_c (m_b-m_c)^4},$$
$$\langle Q_8(J/\psi)\rangle_x = -\frac{8\sqrt{2}\pi f_\pi \psi_{J/\psi}(0)\psi_{B_c}(0)\varphi_\pi(x) P_{B_c}\cdot\varepsilon_\Psi^* C_A C_F \alpha_s (m_b+m_c)^{1/2}}{m_c^{1/2} N_c^2 (m_b-m_c)^2((x-1)m_b+(3x-2)m_c)(xm_b+(3x-1)m_c)} \times (3(2x-1)m_b m_c+(x-1)m_b^2+(9x-4)m_c^2). \tag{10}$$

Note that $\langle Q_8\rangle$ in Eqs. (9) and (10) is not symmetrical when we exchange x with $\bar{x}=1-x$, because of the nonfactorizable (NF) contribution from the axial vector current, which brings in an antisymmetrical part. However, the antisymmetrical part can be easily proved to be insignificant. We define the function $V(x)$ to collect the contributions from the axial vector current, and it satisfies $V(\bar{x})=-V(x)$. Considering the symmetrical pion LCDA, i.e., $\phi_\pi(\bar{x})=\phi_\pi(x)$, we can easily get the result

$$\int_0^1 V(x)\phi_\pi(x)dx = -\int_1^0 V(\bar{x})\phi_\pi(\bar{x})dx = -\int_0^1 V(x)\phi_\pi(x)dx = 0. \tag{11}$$

Furthermore, employing the asymptotic LCDA $\phi_\pi(x,\mu=\infty)=6x\bar{x}$, we can obtain the integrated matrix elements $\langle Q_i\rangle$:

$$\langle Q_0(\eta_c)\rangle = \frac{8\sqrt{2}\pi f_\pi \psi_{\eta_c}(0)\psi_{B_c}(0) C_A C_F \alpha_s \sqrt{m_b+m_c}(m_b+3m_c)(2m_b m_c+3m_b^2+3m_c^2)}{m_c^{3/2} N_c (m_b-m_c)^3},$$
$$\langle Q_8(\eta_c)\rangle = \frac{6\sqrt{2}\pi f_\pi \psi_{\eta_c}(0)\psi_{B_c}(0) C_A C_F \alpha_s \sqrt{m_b+m_c}}{m_c^{3/2} N_c^2 (m_b-m_c)(m_b+3m_c)} \times [2m_b m_c(\ln(m_b+2m_c) - \ln(m_c)+2) + m_c^2(4\ln(m_b+2m_c) - 4\ln(m_c)+3) + m_b^2],$$
$$\langle Q_0(\Psi)\rangle = -\frac{64\sqrt{2}\pi f_\pi \psi_{J/\psi}(0)\psi_{B_c}(0) P_{B_c}\cdot\varepsilon_\Psi^* C_A C_F \alpha_s (m_b+m_c)^{5/2}}{m_c^{1/2} N_c (m_b-m_c)^4},$$
$$\langle Q_8(\Psi)\rangle = -\frac{24\sqrt{2}\pi f_\pi \psi_{J/\psi}(0)\psi_{B_c}(0) P_{B_c}\cdot\varepsilon_\Psi^* C_A C_F \alpha_s (m_b+m_c)^{1/2}}{m_c^{1/2} N_c^2 (m_b-m_c)(m_b+3m_c)^3} \times [2m_b m_c(\ln(m_b+2m_c) - \ln(m_c)+2) + m_c^2(4\ln(m_b+2m_c) - 4\ln(m_c)+3) + m_b^2]. \tag{12}$$

Differently from the traditional formalisms in Refs. [18,22], herein we have extracted the hard kernels T_i from Wilson coefficients separately. And the Wilson coefficients $C_i(\mu)$ contain the contributions from the energy region from m_W to m_b, while the hard kernels $T_i(\mu)$ include the contributions from the energy region below m_b. They can be calculated perturbatively order by order.

$$\begin{aligned}\mathcal{A}(B_c^- \to J/\psi(\eta_c)\pi^-) &= \frac{G_F}{\sqrt{2}} V_{ud}^* V_{cb}(C_0(\mu)T_{f,0}M_f + C_0(\mu)T_{nf,0}M_{nf} \\ &\quad + C_8(\mu)T_{nf,8}M_{nf}),\end{aligned} \tag{13}$$

$$\begin{aligned}T_{f,i}(\mu) &= \sum_{k=0}^{\infty}\left(\frac{\alpha_s}{4\pi}\right)^k T_{f,i}^{(k)}(\mu), \\ T_{nf,i}(\mu) &= \sum_{k=0}^{\infty}\left(\frac{\alpha_s}{4\pi}\right)^k T_{nf,i}^{(k)}(\mu),\end{aligned} \tag{14}$$

where T_f means the factorizable hard kernel, T_{nf} means the nonfactorizable hard kernel, and the Wilson coefficients C_i are

$$C_0 = \frac{2}{3}C_+ + \frac{1}{3}C_-, \qquad C_8 = C_+ - C_-, \tag{15}$$

where

$$\begin{aligned}C_\pm &= \left[\frac{\alpha_s(M_W)}{\alpha_s(\mu)}\right]^{\frac{\gamma_\pm}{2\beta_0}}, \\ \gamma_\pm &= \pm 6\frac{N_c \mp 1}{N_c}, \\ \beta_0 &= \frac{11N_c - 2n_f}{3}.\end{aligned} \tag{16}$$

Fixing $M_f(\eta_c) = \langle Q_0(\eta_c)\rangle$, $M_f(J/\psi) = \langle Q_0(\Psi)\rangle$, $M_{nf}(\eta_c) = \langle Q_8(\eta_c)\rangle$, and $M_{nf}(J/\psi) = \langle Q_8(\Psi)\rangle$, we can extract the leading-order hard kernel $T_i^{(0)}$:

$$\begin{aligned}T_{f,0}^{(0)}(\eta_c) &= T_{f,0}^{(0)}(J/\psi) = 1, \\ T_{nf,0}^{(0)}(\eta_c) &= T_{nf,0}^{(0)}(J/\psi) = 0, \\ T_{nf,8}^{(0)}(\eta_c) &= T_{nf,8}^{(0)}(J/\psi) = 1.\end{aligned} \tag{17}$$

B. Next-to-leading order (NLO)

Now we pay more attention to the NLO correction. The one-loop diagrams for $B_c \to J/\psi(\eta_c)\pi$ are classified in Figs. 2, 3, and 4, where Fig. 2 lays out the one-loop factorizable diagrams, while the nonfactorizable diagrams are shown in Figs. 3 and 4. To regularize the ultraviolet and infrared divergences, we use a dimensional regularization scheme, but we use a relative-velocity regularization scheme for Coulomb divergence. The renormalization

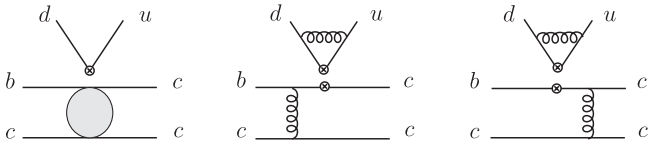

FIG. 2. One-loop factorizable diagrams contribute to $\langle Q_0\rangle$. The bubble in the first diagram expresses all one-loop form-factor diagrams, which are displayed in Refs. [28,29].

constants are listed in Appendix B. In our calculation, the mathematical package FeynArts [23] was used to generate the Feynman diagrams, FeynCalc [24] was used to deal with the amplitudes, and LoopTools [25] was used to calculate the one-loop integrals. The practicable γ_5 scheme is adopted in D-dimensional computation [26,27].

1. $T_0^{(1)}$

The one-loop diagrams that contribute to $\langle Q_0\rangle$ can be distributed into two sets: factorizable (see Fig. 2) and nonfactorizable diagrams (see Fig. 3). And the NLO B_c-to-S-wave-charmonium form factors have been calculated in Refs. [28–30,49]. For the right two diagrams in Fig. 2, their UV divergence can be canceled by external-field counterterms.

We analyze the factorizable part at first. In NF, $\langle Q_8\rangle$ vanishes, and

$$\begin{aligned}\langle J/\psi(\eta_c)\pi^-|Q_0|B_c^-\rangle \approx{}& \langle J/\psi(\eta_c)|\bar{c}\gamma^\mu(1-\gamma_5)b|B_c^-\rangle \\ &\times \langle \pi^-|\bar{d}\gamma_\mu(1-\gamma_5)u|0\rangle,\end{aligned} \tag{18}$$

i.e., $\langle Q_0\rangle$ is proportional to the product of the pion decay constant and the $B_c^- \to J/\psi(\eta_c)$ transition form factor. Conventionally, we adopt the following parameterizations for the decay constants and $B_c^- \to J/\psi(\eta_c)$ transition form factors:

$$\langle \pi^-(p')|\bar{d}\gamma_\mu\gamma_5 u|0\rangle = -if_\pi p'_\mu, \tag{19}$$

$$\begin{aligned}\langle \eta_c(p)|\bar{c}\gamma^\mu b|B_c^-(P)\rangle ={}& f_+(q^2)\left[P^\mu + p^\mu - \frac{m_{B_c}^2 - m_{\eta_c}^2}{q^2}q^\mu\right] \\ &+ f_0(q^2)\frac{m_{B_c}^2 - m_{\eta_c}^2}{q^2}q^\mu,\end{aligned} \tag{20}$$

$$\langle J/\psi(p,\varepsilon^*)|\bar{c}\gamma^\mu b|B_c^-(P)\rangle = \frac{2iV(q^2)}{m_{B_c} + m_{J/\psi}}\varepsilon^{\mu\nu\rho\sigma}\varepsilon_\nu^* p_\rho P_\sigma, \tag{21}$$

$$\begin{aligned}&\langle J/\psi(p,\varepsilon^*)|\bar{c}\gamma^\mu\gamma_5 b|B_c^-(P)\rangle \\ &\quad= 2m_{J/\psi}A_0(q^2)\frac{\varepsilon^*\cdot q}{q^2}q^\mu + (m_{B_c} + m_{J/\psi})A_1(q^2) \\ &\qquad\times\left[\varepsilon^{*\mu} - \frac{\varepsilon^*\cdot q}{q^2}q^\mu\right] - A_2(q^2)\frac{\varepsilon^*\cdot q}{m_{B_c} + m_{J/\psi}} \\ &\qquad\times\left[P^\mu + p^\mu - \frac{m_{B_c}^2 - m_{J/\psi}^2}{q^2}q^\mu\right].\end{aligned} \tag{22}$$

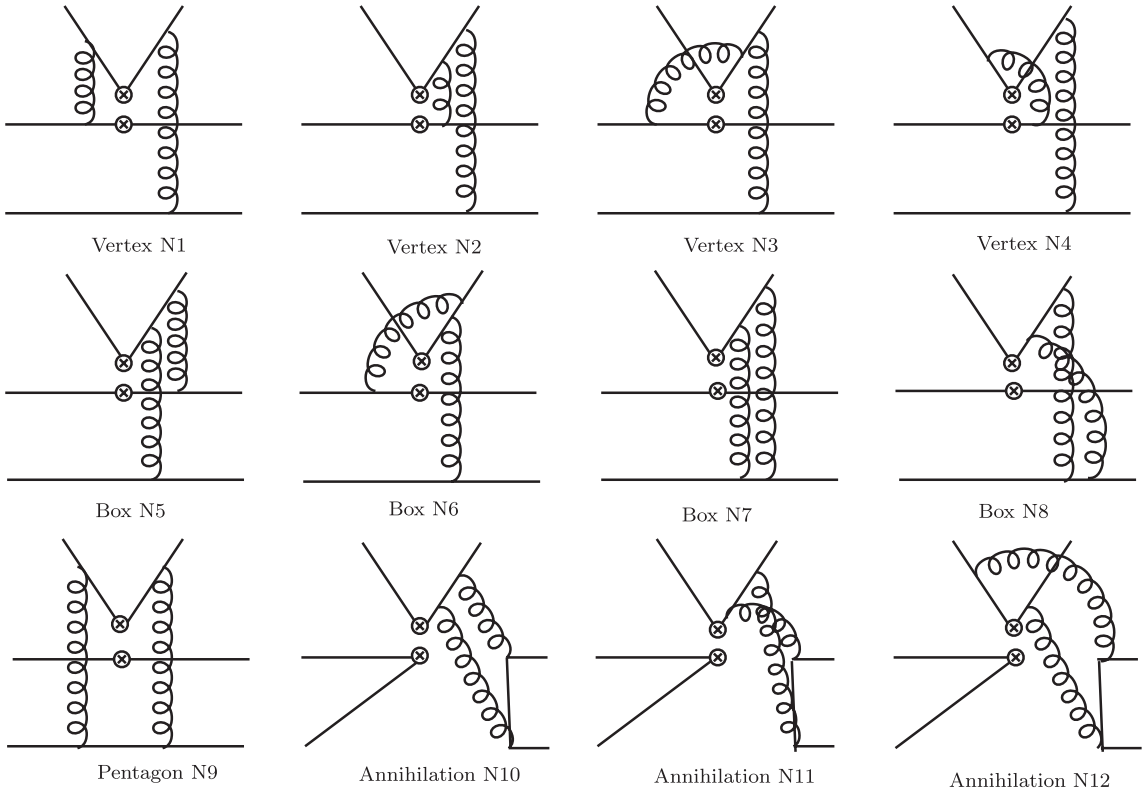

FIG. 3. Twelve of 24 one-loop nonfactorizable diagrams contribute to $\langle Q_0 \rangle$. The other 12 partners can be obtained by interchanging the u and d quarks. Note that the diagrams from N1 to N9 also contribute to $\langle Q_8 \rangle$.

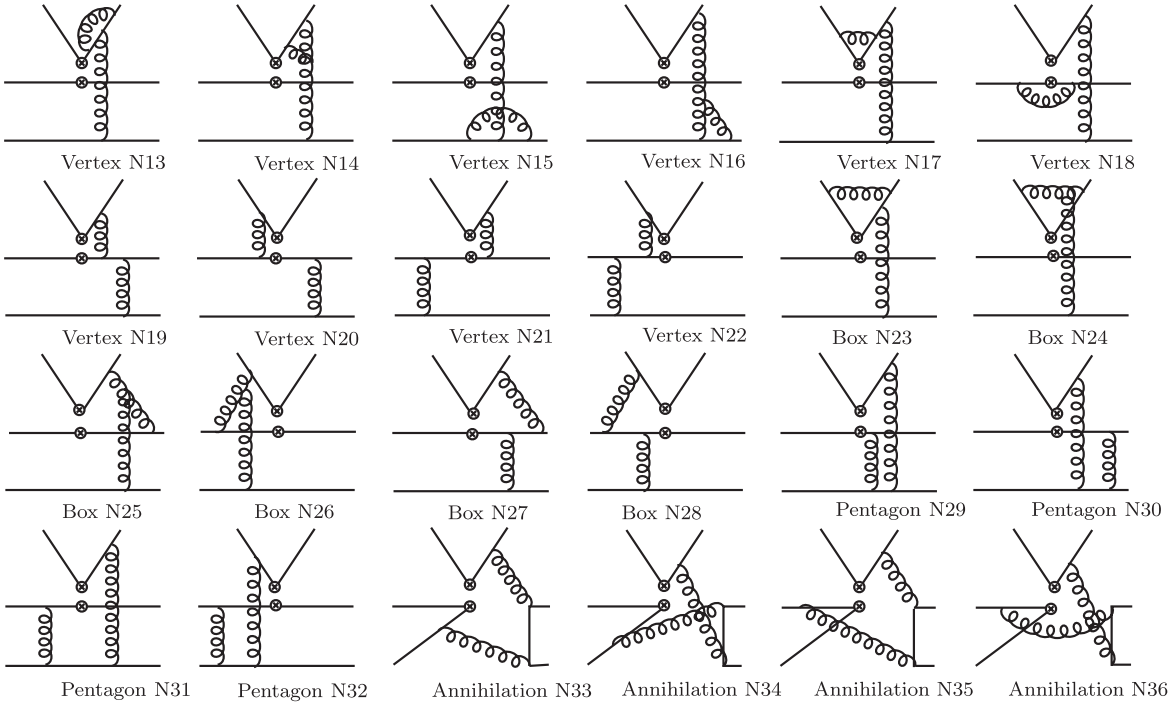

FIG. 4. Twenty-four of the 65 one-loop nonfactorizable diagrams contribute to $\langle Q_8 \rangle$. Another 23 diagrams can be obtained by interchanging the u and d quarks, and the left 18 come from the diagrams Vertex N1 to Pentagon N9 in Fig. 3 and their symmetrical partners.

Here we define momentum transfer $q = P - p$ and $\epsilon^{0123} = -1$. Note that $f_0(0) = f_+(0)$.

The tree-level form factors can be obtained easily. They read

$$f_+^{\mathrm{LO}}(q^2) = \frac{8\sqrt{2}C_A C_F \pi\sqrt{z+1}\left(-\frac{q^2}{m_b^2} + 3z^2 + 2z + 3\right)\alpha_s \psi(0)_{B_c}\psi(0)_{\eta_c}}{\left(\frac{q^2}{m_b^2} - (z-1)^2\right)^2 z^{3/2} m_b^3 N_c}, \tag{23}$$

$$f_0^{\mathrm{LO}}(q^2) = \frac{8\sqrt{2}C_A C_F \pi\sqrt{z+1}(9z^3 + 9z^2 + 11z - \frac{q^2}{m_b^2}(5z+3) + 3)\alpha_s \psi(0)_{B_c}\psi(0)_{\eta_c}}{\left(\frac{q^2}{m_b^2} - (z-1)^2\right)^2 z^{3/2}(3z+1) m_b^3 N_c}, \tag{24}$$

$$V^{\mathrm{LO}}(q^2) = \frac{16\sqrt{2}C_A C_F \pi(3z+1)\alpha_s \psi(0)_{B_c}\psi(0)_{J/\psi}}{\left(\frac{q^2}{m_b^2} - (z-1)^2\right)^2 \left(\frac{z}{z+1}\right)^{3/2} m_b^3 N_c}, \tag{25}$$

$$A_0^{\mathrm{LO}}(q^2) = \frac{16\sqrt{2}C_A C_F \pi(z+1)^{5/2}\alpha_s \psi(0)_{B_c}\psi(0)_{J/\psi}}{\left(\frac{q^2}{m_b^2} - (z-1)^2\right)^2 z^{3/2} m_b^3 N_c}, \tag{26}$$

$$A_1^{\mathrm{LO}}(q^2) = \frac{16\sqrt{2}C_A C_F \pi\sqrt{z+1}(4z^3 + 5z^2 + 6z - \frac{q^2}{m_b^2}(2z+1) + 1)\alpha_s \psi(0)_{B_c}\psi(0)_{J/\psi}}{\left(\frac{q^2}{m_b^2} - (z-1)^2\right)^2 z^{3/2}(3z+1) m_b^3 N_c}, \tag{27}$$

$$A_2^{\mathrm{LO}}(q^2) = \frac{16\sqrt{2}C_A C_F \pi\sqrt{z+1}(3z+1)\psi(0)_{B_c}\psi(0)_{J/\psi}}{\left(\frac{q^2}{m_b^2} - (z-1)^2\right)^2 z^{3/2} m_b^3 N_c}, \tag{28}$$

here $z \equiv m_c/m_b$.

When neglecting the mass of the pion, we have the factorizable contribution in NF:

$$\begin{aligned} \langle \eta_c \pi^- | Q_{0,f} | B_c^- \rangle &= i f_\pi f_0(0)(m_{B_c}^2 - m_{\eta_c}^2), \\ \langle J/\psi \pi^- | Q_{0,f} | B_c^- \rangle &= -i f_\pi A_0(0)(m_{B_c}^2 - m_{J/\psi}^2), \end{aligned} \tag{29}$$

where we have used the fact that J/ψ is longitudinally polarized, so that

$$2m_{J/\psi}\varepsilon^* \cdot P = 2m_{B_c}|\vec{p}_c| = m_{B_c}^2 - m_{J/\psi}^2.$$

Therefore, we have the LO result

$$\langle \eta_c \pi^- | Q_0 | B_c^- \rangle^{\mathrm{LO}} = i\frac{8\sqrt{2}\pi\alpha_s C_A C_F\sqrt{z+1}(9z^3 + 9z^2 + 11z + 3) f_\pi \psi(0)_{B_c}\psi(0)_{\eta_c}}{(1-z)^3 z^{3/2} m_b N_c}, \tag{30}$$

and in the heavy quark limit $z \to 0$, we have

$$\lim_{z\to 0}\langle\eta_c\pi^-|Q_0|B_c^-\rangle^{\rm LO}=i\frac{24\sqrt{2}\pi\alpha_s C_A C_F f_\pi\psi(0)_{B_c}\psi(0)_{\eta_c}}{z^{3/2}m_b N_c}. \tag{31}$$

Actually, the approximation above is not so good. Numerically, we have

$$\left.\frac{\lim_{z\to 0}\langle\eta_c\pi^-|Q_0|B_c^-\rangle^{\rm LO}}{\langle\eta_c\pi^-|Q_0|B_c^-\rangle^{\rm LO}}\right|_{z=1.5/4.8}\approx 0.11, \tag{32}$$

which is essentially bad. The perturbative series expanded as Eq. (13), however, can resolve the problem, because the convergence of hard kernel T_i is well behaved.

Note that the complete analytic expression is too lengthy to present, and it is possible to derive an asymptotic analytic formula valid in phenomenological application. Thus, we present our results in the heavy quark limit, i.e., $m_b\to\infty$.

The factorizable hard kernel $T_{f,0}^{(1)}$ is identical to the ratio of the NLO form factor to the tree-level one:

$$\begin{aligned}T_{f,0}^{(1)}(\eta_c)&=\frac{f_0^{(1)}(0)}{f_0^{(0)}(0)}\\&=\frac{1}{3}(11C_A-2n_f)\ln\left(\frac{2\mu^2}{zm_b^2}\right)-\frac{10n_f}{9}-\frac{1}{3}\ln z-\frac{2\ln 2}{3}+C_F\left(\frac{1}{2}\ln^2 z+\frac{10}{3}\ln 2\ln z-\frac{35}{6}\ln z+\frac{2\ln^2 2}{3}\right.\\&\left.+3\ln 2+\frac{7\pi^2}{9}-\frac{103}{6}\right)+C_A\left(-\frac{1}{6}\ln^2 z-\frac{1}{3}\ln 2\ln z-\frac{1}{3}\ln z+\frac{\ln^2 2}{3}-\frac{4\ln 2}{3}-\frac{5\pi^2}{36}+\frac{73}{9}\right),\end{aligned} \tag{33}$$

$$\begin{aligned}T_{f,0}^{(1)}(\Psi)&=\frac{A_0^{(1)}(0)}{A_0^{(0)}(0)}\\&=\frac{1}{3}(11C_A-2n_f)\ln\left(\frac{2\mu^2}{zm_b^2}\right)-\frac{10n_f}{9}+C_F\left(\frac{1}{2}\ln^2 z-\frac{119}{8}+7\ln 2\ln z-\frac{21}{4}\ln z+7\ln^2 2+\frac{15\ln 2}{4}\right)\\&+C_A\left(-\frac{3}{8}\ln^2 z-\ln 2\ln z-\frac{9}{8}\ln z-\frac{7\pi^2}{24}+\frac{67}{9}-\frac{9\ln^2 2}{4}+\frac{3\ln 2}{8}\right).\end{aligned} \tag{34}$$

Next, we turn to the nonfactorizable part. There are 24 one-loop nonfactorizable diagrams that contribute to $\langle Q_0\rangle$, half of which are displayed in Fig. 3. The corresponding color factors are summed up in Table I. Over 100 of the one-loop integrals in Figs. 3 and 4 are created, and they can be reduced into master integrals (MIs) and some two-point Passarino-Veltman integrals [25]. Our analytic expressions of MIs are in agreement with what is given in Refs. [31,32].

The numerical one-loop nonfactorizable contributions for $T_{nf,0}^{(1)}$ are

$$T_{nf,0}^{(1)}(\eta_c)=6\ln\left(\frac{m_b^2}{\mu^2}\right)+16.75, \tag{35}$$

$$T_{nf,0}^{(1)}(\Psi)=T_{nf,0}^{(1)}(\eta_c). \tag{36}$$

And the complete results in the heavy quark limit can be found in Appendix C.

2. $T_8^{(1)}$

Here, we study the one-loop nonfactorizable contributions to $\langle Q_8\rangle$. Twenty-four diagrams are shown in Fig. 4, another nine diagrams are collected in Fig. 3 from N1 to N9, and the rest can be obtained by interchanging the u and d quarks. The corresponding color factors are summed up in Tables I and II.

TABLE I. Color factors of the corresponding diagrams in Fig. 3. Therein, the figures from N1 to N9 contribute not only $\langle Q_0\rangle$, but also $\langle Q_8\rangle$.

Diagram	N1–2, N6, N8–9	N3–5, N7	N10–12
Color in $\langle Q_8\rangle$	$\frac{(C_A^2-2)C_F}{4}$	$-\frac{C_F}{2}$	0
Color in $\langle Q_0\rangle$		$\frac{C_A C_F}{2}$	

TABLE II. Color factors of the corresponding diagrams in Fig. 4. They contribute only to $\langle Q_8\rangle$.

Diagram	N13, N15, N17–18, N27–29, N33–36	N14, N26	N16, N24–25	N19–23, N30–32
Color in $\langle Q_8\rangle$	$\frac{2C_A C_F}{3}$	$\frac{iC_A^2 C_F}{4}$	$-\frac{iC_A^2 C_F}{4}$	$-\frac{C_A C_F}{12}$

After integrating the fraction, we have the corresponding $T^{(1)}_{nf,8}$:

$$T^{(1)}_{nf,8}(\eta_c) = \frac{1}{3}(-11C_A + 2n_f + 16N_c - 6)\ln\left(\frac{m_b^2}{\mu^2}\right) - \frac{12.48}{N_c} + (9\ln z + 1)C_F - \left(\frac{\ln^2 z}{2} - \frac{6\ln 2 - 23}{3}\ln z + 278.1\right)C_A - \frac{2}{9}n_f(-3\ln z + 5 + 3\ln 2) + \frac{\ln^2 z}{6} - \frac{8(3+\ln 2)}{3}\ln z + 548.9, \quad (37)$$

$$T^{(1)}_{nf,8}(\Psi) = \frac{1}{9}(-33C_A + 6n_f + 32N_c - 18)\ln\left(\frac{m_b^2}{\mu^2}\right) - \frac{12.48}{N_c} + (9\ln z + 1)C_F - \left(\frac{\ln^2 z}{2} - \frac{6\ln 2 - 23}{3}\ln z + 278.1\right)C_A - \frac{2}{9}n_f(-3\ln z + 5 + 3\ln 2) + \frac{\ln^2 z}{6} - \frac{8(3+\ln 2)}{3}\ln z + 542.3. \quad (38)$$

IV. THE PHENOMENOLOGICAL STUDIES

The decay width can be written as

$$\Gamma(B_c \to J/\psi(\eta_c)\pi) = \frac{|p|}{8\pi m_{B_c}^2}|\mathcal{A}(B_c \to J/\psi(\eta_c)\pi)|^2. \quad (39)$$

Here, the momentum of final particle satisfies $|p| = (m_{B_c}^2 - m_\Psi^2)/2m_{B_c}$ in the B_c-meson rest frame, and we adopt the input parameters as below [33]:

$$m_c = 1.4 \pm 0.1\ \text{GeV}, \quad m_b = 4.9 \pm 0.1\ \text{GeV},$$
$$\Lambda_{\rm QCD} = 100\ \text{MeV}, \quad G_F = 1.16637 \times 10^{-5}\ \text{GeV}^{-2},$$
$$|V_{ud}^* V_{cb}| = A\lambda^2(1 - \lambda^2/2 - \lambda^4/8),$$
$$n_f = 3, \quad N_c = 3, \quad C_F = 4/3,$$
$$|V_{us}^*| = 0.2252, \quad |V_{cb}| = 0.0406,$$
$$f_\pi = 130.4\ \text{MeV}, \quad f_\rho = 216\ \text{MeV},$$
$$f_K = 156.1\ \text{MeV}, \quad f_{K^*} = 220\ \text{MeV},$$

where $A = 0.814$, $\lambda = 0.2257$. The Schrödinger wave function at the origin for J/ψ is determined through its leptonic decay width, $\Gamma^\psi_{ee} = 5.55$ keV[33]. Numerically, we can obtain $|\psi^{\rm LO}_\Psi(0)|^2 = 0.0447\ (\text{GeV})^3$ and $|\psi^{\rm NLO}_\Psi(0)|^2 = 0.0801\ (\text{GeV})^3$. For that of B_c, we shall determine its value to be $|\psi_{B_c}(0)|^2 = 0.1307\ (\text{GeV})^3$, which is derived under the Buchmüller-Tye potential [34]. Besides, the one-loop result for the strong coupling constant is used, i.e.,

$$\alpha_s(\mu) = \frac{4\pi}{(11 - \frac{2}{3}n_f)\ln\left(\frac{\mu^2}{\Lambda^2_{\rm QCD}}\right)}.$$

Within the above input parameters, we can obtain the decay width of B_c decays to S-wave charmonium and pions at NLO accuracy. In practice, the renormalization scale μ may run from $2m_c$ to m_b, and the μ dependence of the branching ratio is shown in Fig. 5. Therein, we plot both kinds of NLO results: one letting $m_c/m_b \to 0$ in the heavy quark limit, and the other fixing the ratio m_c/m_b to its physical value. The first one is valid in leading m_c/m_b, while the latter is summed to all orders of m_c/m_b. It turns

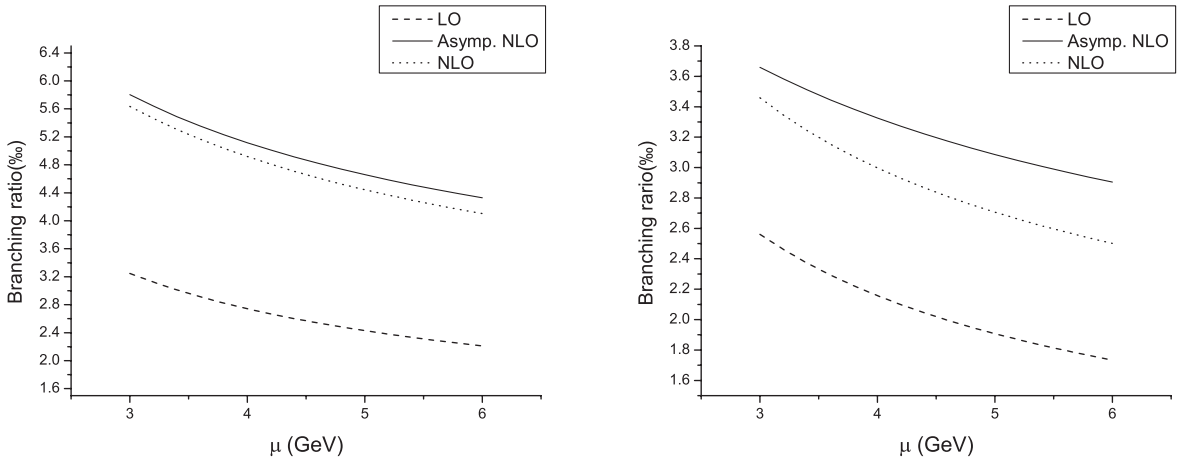

FIG. 5. The branching ratios of $B_c \to \eta_c\pi$ (left) and $B_c \to J/\psi\pi$ (right) vs the renormalization scale μ. Herein $m_c = 1.5$ GeV, $m_b = 4.8$ GeV, and for the lifetime of the B_c we take $\tau(B_c) = 0.453$ ps. The results for LO, asymptotic NLO, and complete NLO are shown.

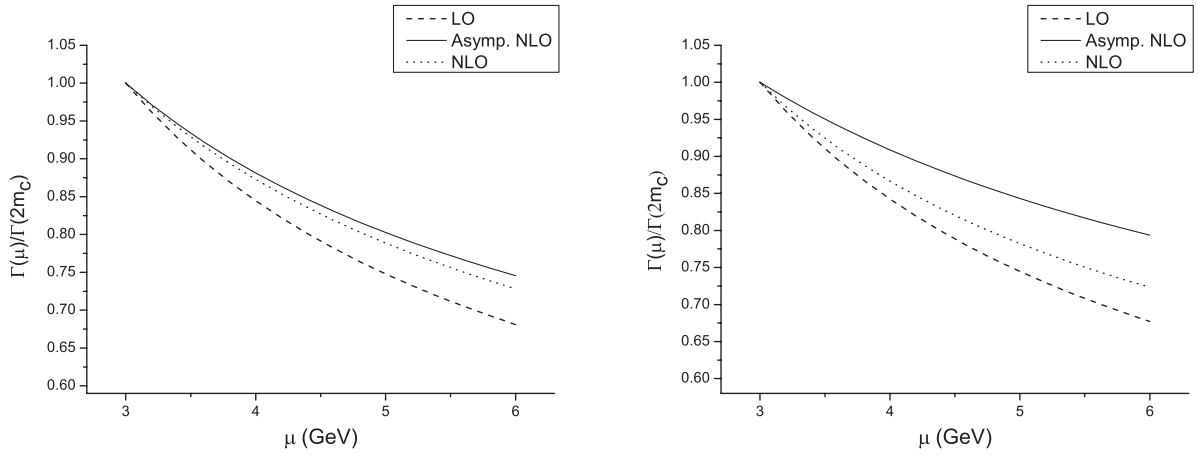

FIG. 6. The ratios $\Gamma(\mu)/\Gamma(2m_c)$ of $B_c \to \eta_c\pi$ (left) and $B_c \to J/\psi\pi$ (right) vs the renormalization scale μ. Herein $m_c = 1.5$ GeV, $m_b = 4.8$ GeV.

out that the leading-order approximation in the m_c/m_b expansion, namely the asymptotic NLO result, accounts for more than 85% of the complete NLO result. That means that it is enough for us to use this simple and analytic expression for phenomenological studies in the place of the complicated NLO expression. The NLO corrections can reduce the uncertainty, which is explicitly exhibited in Fig. 6.

Apart from the uncertainty of the renormalization scale, we also study the uncertainty from the quark mass. We find that both of them are important for the final results. The vivid figures considering both dependences are drawn in Fig. 7, in which we also detail the influences from Gegenbauer polynomials of the light-cone distribution amplitude of the pion; however, these bring about a slight influence on the final result.

After considering the uncertainties stated above, we give out our results based on NRQCD factorization in Table III and compare them with those calculated from other models. The LO results are generally close to the results of the QCD sum rule [35,36], the constituent quark model [37–40] and the light-front ISGW model [41]; however, they are larger than those of the relativistic potential model [42] and the relativistic quark model [43]. Our work showed that the NLO corrections substantially enhance the branching ratios, and the NLO QCD correction K factors are $1.75^{+0.14+0.18}_{-0.34-0.11}$ for $\Gamma(B_c \to \eta_c\pi)$ and $1.31^{+0.06+0.18}_{-0.18-0.12}$ for $\Gamma(B_c \to J/\psi\pi)$.

Moreover, we want to study the degree of importance for the factorizable part at NLO accuracy. After calculation, we find that the asymptotic factorizable contribution can be well-represented by the majority of the branching ratio. To present it more vividly, let us set $m_c = 1.4$ GeV, $m_b = 4.9$ GeV, and $\mu = 3$ GeV, and we obtain

$$\begin{aligned} \mathrm{Br}(B_c \to \eta_c\pi)^{\text{Asymp. factorizable}} &= 5.10‰, \\ \mathrm{Br}(B_c \to \eta_c\pi)^{\text{total}} &= 5.20‰, \\ \mathrm{Br}(B_c \to J/\psi\pi)^{\text{Asymp. factorizable}} &= 3.06‰, \\ \mathrm{Br}(B_c \to J/\psi\pi)^{\text{total}} &= 2.91‰. \end{aligned} \tag{40}$$

Experimentally, the pp collisions at the LHC have been performed at a center-of-mass energy of $\sqrt{s} = 8$ TeV, and

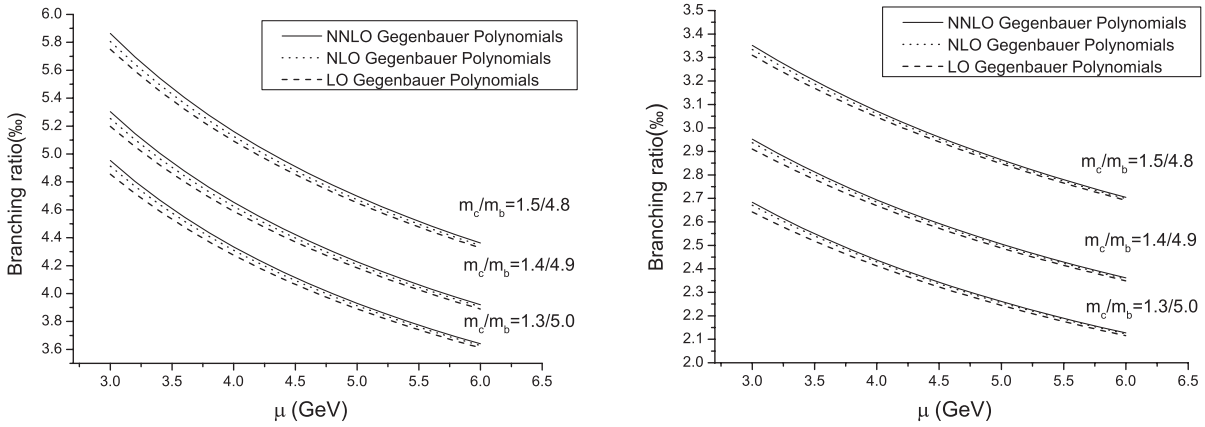

FIG. 7. The branching ratios of $B_c \to \eta_c\pi$ (left) and $B_c \to J/\psi\pi$ (right) vs the renormalization scale μ, for different choices of quark mass. LO, NLO, and NNLO Gegenbauer polynomials of Pion's light-cone distribution amplitude are considered in turn.

TABLE III. Branching ratios (in ‰) of exclusive nonleptonic B_c decays into S-wave charmonium states. For the lifetime of the B_c, we take $\tau(B_c) = 0.453$ ps. In our work, we choose the quantities $m_c = 1.4$ GeV, $m_b = 4.9$ GeV, and $\mu = 3$ GeV. The uncertainty in the first column of the value is from varying the renormalization scale μ from 2.5 GeV to 5 GeV, while the uncertainty in the second column comes from varying the quark mass m_c/m_b from 1.5/4.8 to 1.3/5.0.

Mode	This work (NLO)	LO	[35,36]	[37]	[41]	[42]	[43]	[38]	[39]	[40]
$B_c^+ \to \eta_c\pi^+$	$5.19^{+0.44+0.55}_{-1.01-0.34}$	2.95	2.0	2.2	1.3	0.26	0.85	1.4	1.9	2.1
$B_c^+ \to \eta_c\rho^+$	$14.5^{+1.29+1.53}_{-2.92-0.95}$	7.89	4.2	5.9	3.0	0.67	2.0	3.3	4.5	⋯
$B_c^+ \to \eta_c K^+$	$0.38^{+0.03+0.04}_{-0.07-0.02}$	0.21	0.13	0.17	0.13	0.02	0.06	0.11	0.15	⋯
$B_c^+ \to \eta_c K^{*+}$	$0.77^{+0.07+0.08}_{-0.16-0.05}$	0.41	0.20	0.31	0.21	0.04	0.11	0.18	0.25	⋯
$B_c^+ \to J/\psi\pi^+$	$2.91^{+0.15+0.40}_{-0.42-0.27}$	2.22	1.3	2.1	0.73	1.3	0.61	1.1	1.7	2.0
$B_c^+ \to J/\psi\rho^+$	$8.08^{+0.45+1.09}_{-1.21-0.73}$	6.03	4.0	6.5	2.1	3.7	1.6	3.1	4.9	⋯
$B_c^+ \to J/\psi K^+$	$0.22^{+0.01+0.03}_{-0.03-0.02}$	0.16	0.11	0.16	0.07	0.07	0.05	0.08	0.13	⋯
$B_c^+ \to J/\psi K^{*+}$	$0.43^{+0.02+0.06}_{-0.07-0.04}$	0.32	0.22	0.35	0.16	0.20	0.10	0.18	0.28	⋯
$B_c^+ \to \psi(2S)\pi^+$	$0.76^{+0.04+0.10}_{-0.11-0.07}$	0.58	⋯	0.27	⋯	0.19	0.11	⋯	⋯	⋯
$B_c^+ \to \psi(2S)\rho^+$	$2.11^{+0.12+0.28}_{-0.32-0.19}$	1.57	⋯	0.77	⋯	0.48	0.18	⋯	⋯	⋯
$B_c^+ \to \psi(2S)K^+$	$0.057^{+0.003+0.008}_{-0.008-0.005}$	0.042	⋯	0.019	⋯	0.009	0.01	⋯	⋯	⋯
$B_c^+ \to \psi(2S)K^{*+}$	$0.112^{+0.005+0.015}_{-0.018-0.010}$	0.083	⋯	0.041	⋯	0.026	0.01	⋯	⋯	⋯

the energy will arrive at $\sqrt{s} = 14$ TeV in the future. pp collisions provide a mass production source for B_c mesons. Since the B_c^* decays into the B_c with a probability of almost 100%, including the contributions from the S-wave excited states, the cross section of the B_c meson at LHC was estimated to be around 10^2 nb. With 10 fb^{-1} of integrated luminosity, there are around 10^9 events for B_c production. In that case, the measurements of $B_c \to J/\psi\pi \to \mu^+\mu^-\pi$ and $B_c \to J/\psi\pi \to e^+e^-\pi$ are feasible, and the events are presented in Table IV, in which we have considered the quark mass dependence.

Finally, let us study some specific channels which have been measured by the LHCb Collaboration recently. The LHCb Collaboration have measured $\mathrm{Br}(B_c^+ \to J/\psi\pi^+\pi^-\pi^+)/\mathrm{Br}(B_c^+ \to J/\psi\pi^+)$ to be $2.41 \pm 0.30 \pm 0.33$, using 0.8 fb^{-1} data of pp collisions at a center-of-mass energy of $\sqrt{s} = 7$ TeV [8]. Experimentally, the reconstructed invariant mass distribution of the $\pi^+\pi^-\pi^+$ combinations favors a resonance state $a_1^+(1260)$.

In theoretical aspects, there are mainly two channels which contribute to the signal of $B_c^+ \to J/\psi\pi^+\pi^-\pi^+$: $B_c^+ \to J/\psi a_1^+(1260)$ followed by $a_1^+(1260) \to \pi^+\pi^-\pi^+$, and $B_c^+ \to \Psi(2S)\pi^+$ followed by $\Psi(2S) \to J/\psi\pi^+\pi^-$. Practically, $\mathrm{Br}(B_c^+ \to \Psi(2S)\pi^+)/\mathrm{Br}(B_c^+ \to J/\psi\pi^+) = (A_0^2(0)_{\Psi(2S)}(m_{B_c}^2 - m_{\psi(2S)}^2)^3)/(A_0^2(0)_{\Psi}(m_{B_c}^2 - m_{\psi}^2)^3) \approx 0.26$, and $\mathrm{Br}(\Psi(2S) \to J/\psi\pi^+\pi^-) = 33.6\%$ [33]. So the contribution to $\mathrm{Br}(B_c^+ \to J/\psi\pi^+\pi^-\pi^+)/\mathrm{Br}(B_c^+ \to J/\psi\pi^+)$ from $\Psi(2S)$ is 0.08, which explains the experimental data that favor the resonance state $a_1^+(1260)$ rather than $\Psi(2S)$.

In the former section, we have performed a complete QCD NLO calculation of B_c decays into S-wave charmonia and light mesons. And we found that the factorizable contributions account for more than 85% of the total results at NLO accuracy in the heavy quark limit as Eq. (40). Here we assume that this also holds in $B_c^+ \to J/\psi a_1^+(1260)$; i.e., it can reserve a high accuracy just from considering the factorizable diagrams. So we adopt the naive factorization scheme. And for the axial-vector meson $a_1^+(1260)$, the matrix element for its creation is

$$\langle a_1^+(1260)(p,\epsilon^*)|\bar{u}\gamma_\mu\gamma_5 d|0\rangle = -if_{a_1}m_{a_1}\epsilon_\mu^*. \quad (41)$$

TABLE IV. The events of $B_c \to J/\psi\pi \to \mu^+\mu^-\pi$, $B_c \to J/\psi\pi \to e^+e^-\pi$ and $B_c \to \eta_c\pi \to \gamma\gamma\pi$ with 10 fb^{-1} data, using various values of the c-quark mass m_c and fixed b-quark mass $m_b = 4.8$ GeV.

	Tevatron ($\sqrt{S} = 2$.TeV)					LHC ($\sqrt{S} = 14$.TeV)				
m_c (GeV)	1.4	1.5	1.6	1.7	1.8	1.4	1.5	1.6	1.7	1.8
σ_{B_c} (nb)	13.4	10.5	8.48	6.89	5.63	214	160	139	114	95.1
$\mu^+\mu^-\pi(\times 10^4)$	2.54	2.15	1.79	1.56	1.40	40.6	32.8	29.3	25.9	23.6
$e^+e^-\pi(\times 10^4)$	2.54	2.15	1.79	1.57	1.40	40.6	32.8	29.3	26.0	23.7
$\gamma\gamma\pi$	47	37	32	27	24	754	567	525	459	413

TABLE V. Branching fraction ratio in comparison with the LHCb data.

Ratio	Our work	LHCb
$\mathrm{Br}(B_c^+ \to J/\psi\pi^+\pi^-\pi^+)/\mathrm{Br}(B_c^+ \to J/\psi\pi^+)$	2.85	$2.41 \pm 0.30 \pm 0.33$ [8]
$\mathrm{Br}(B_c^+ \to J/\psi K^+)/\mathrm{Br}(B_c^+ \to J/\psi\pi^+)$	0.075	$0.069 \pm 0.019 \pm 0.005$ [9]
$\mathrm{Br}(B_c^+ \to \Psi(2S)\pi^+)/\mathrm{Br}(B_c^+ \to J/\psi\pi^+)$	0.260	$0.250 \pm 0.068 \pm 0.014 \pm 0.006$ [10]
$\mathrm{Br}(B_c^+ \to \Psi(2S)K^+)/\mathrm{Br}(B_c^+ \to J/\psi\pi^+)$	0.02	…
$\mathrm{Br}(B_c^+ \to J/\psi\rho^+)/\mathrm{Br}(B_c^+ \to J/\psi\pi^+)$	2.77	…
$\mathrm{Br}(B_c^+ \to J/\psi K^{*+})/\mathrm{Br}(B_c^+ \to J/\psi\pi^+)$	0.147	…

Then we can obtain the ratio

$$\frac{\mathrm{Br}(B_c^+ \to J/\psi a_1^+(1260))}{\mathrm{Br}(B_c^+ \to J/\psi\pi^+)} = \frac{f_{a_1}^2\lambda_0}{f_\pi^2 A_0^2(0)}[\lambda_1 A_1^2(m_{a_1}^2) + \lambda_2 A_2^2(m_{a_1}^2) + \lambda_3 A_1(m_{a_1}^2)A_2(m_{a_1}^2) - \lambda_4 V^2(m_{a_1}^2)],$$

with

$$\lambda_0 = \frac{\sqrt{(m_{a_1}^2 + m_{B_c}^2 - m_\psi^2)^2 - 4m_{a_1}^2 m_{B_c}^2}}{4m_\psi^2(m_{B_c} + m_\psi)^2(m_{B_c}^2 - m_\psi^2)^3}, \quad (42)$$

$$\lambda_1 = (m_{B_c} + m_\psi)^4(-2m_{a_1}^2(m_{B_c}^2 - 5m_\psi^2) + m_{a_1}^4 + (m_{B_c}^2 - m_\psi^2)^2), \quad (43)$$

$$\lambda_2 = (-2m_{a_1}^2(m_{B_c}^2 + m_\psi^2) + m_{a_1}^4 + (m_{B_c}^2 - m_\psi^2)^2)^2, \quad (44)$$

$$\lambda_3 = 2(m_{B_c} + m_\psi)^2(m_{a_1}^2 - m_{B_c}^2 + m_\psi^2)(m_{a_1}^2 - (m_{B_c} - m_\psi)^2) \times (m_{a_1}^2 - (m_{B_c} + m_\psi)^2), \quad (45)$$

$$\lambda_4 = -8m_{a_1}^2 m_\psi^2(-2m_{a_1}^2(m_{B_c}^2 + m_\psi^2) + m_{a_1}^4 + (m_{B_c}^2 - m_\psi^2)^2). \quad (46)$$

According to Ref. [44], we assume that $\mathrm{Br}(a_1^+(1260) \to \pi^+\pi^-\pi^+)$ is equal to $\mathrm{Br}(a_1^+(1260) \to \pi^+\pi^0\pi^0)$ and its value is 50%. We take the input parameters $f_{a_1} = 0.22$ GeV from the QCD sum rules [45] and $m_{a_1} = 1.23$ GeV from the Particle Data Group [33]. The final result is

$$\frac{\mathrm{Br}(B_c^+ \to J/\psi\pi^+\pi^-\pi^+)}{\mathrm{Br}(B_c^+ \to J/\psi\pi^+)} = 2.85^{+0.03+0.18}_{-0.05-0.13}.$$

The uncertainty in the first column of our result comes from the renormalization scale between 2.5 GeV to 6 GeV, while the uncertainty in the second column comes from varying the quark mass m_c/m_b from 1.5/4.8 to 1.3/5.0. It is compatible with the experimental data $2.41 \pm 0.30 \pm 0.33$ when considering its uncertainty. This channel is also studied through W^* conversion in QCD factorization by Likhoded and Luchinsky [46], where the ratio is predicted to be from 1.9 to 2.3.

In order to conveniently compare with the LHCb's data, we present our prediction and experimental data in Table V. For the former three channels, our results can explain the data perfectly, while for the latter three channels, more data is needed to investigate the validity of NRQCD factorization on B_c decays.

V. CONCLUSIONS

We have performed a comprehensive NLO analysis for the B_c meson decays into S-wave charmonia and light mesons such as π, ρ, K and K^*. The NLO QCD correction provides a large K factor, which substantially enhances the branching ratio, while the μ dependence is reduced correspondingly. Considering uncertainties of sorts of input parameters, we find out that the largest uncertainty comes from the masses of bottom and charm quarks.

In the heavy quark limit, the analytic amplitude up to NLO accuracy is derived. Therein, the logarithm $\ln z$ with $z = m_c/m_b$ is absent in the contribution for the color-singlet operator, while this kind of logarithm along with double logarithm $\ln^2 z$ emerges in that of the color-octet operator. And the asymptotic NLO result where we only reserve the leading order in the z expansion can account for more than 85% of the complete NLO result in which z is fixed to its physical value. Therefore, it is helpful for us to use the asymptotic formulas for phenomenological studies.

Numerical results show that the latest LHCb data on B_c decays can be explained perfectly using NRQCD factorization under their corresponding uncertainties. We have also predicted another three channels which shall be checked in the upcoming data. The large branching ratio and the clear signal of final states make it reliable for the measurement of the absolute branching ratios for the processes $B_c \to J/\psi\pi$, $B_c \to J/\psi\rho$, and $B_c \to J/\psi K$ within the updated LHCb data.

ACKNOWLEDGMENTS

This work was supported in part by the National Natural Science Foundation of China (NSFC) under Grants No. 10935012, No. 11121092, No. 11375200, No. 11275263, and No. 11175249.

APPENDIX A: LCDA FOR LIGHT MESONS AND PROJECTION OPERATORS FOR HEAVY QUARKONIA

Considering the twist-2 and twist-3 light-cone distribution amplitudes for the pion, we have the matrix element of the quark's hadronization projection operator [47]

$$\bar{u}_{\alpha a}(xP)\Gamma(x,\ldots)_{\alpha\beta,ab,\ldots}v_{\beta b}(\bar{x}P) \to \frac{if_\pi}{4N_c}\int_0^1 dx M^\pi(x)_{\alpha\beta}\Gamma(x,\ldots)_{\alpha\beta,aa,\ldots}, \tag{A1}$$

with the decay constant $f_\pi = 130.4$ MeV, $\bar{x} = 1-x$, and

$$M^\pi(x)_{\alpha\beta} = \left\{P\gamma_5\phi(x) - \mu_\pi\gamma_5\left(\phi_p(x) - i\sigma_{\mu\nu}n_-^\mu v^\nu\frac{\phi'_\sigma(x)}{6} + i\sigma_{\mu\nu}P^\mu\frac{\phi_\sigma(x)}{6}\frac{\partial}{\partial k_{\perp\nu}}\right)\right\}_{\alpha\beta}. \tag{A2}$$

Here $\mu_\pi = m_\pi^2/(m_u+m_d)$, $n_\pm$ are light-cone vectors, $\phi(x)$ is the twist-2 distribution amplitude, and $\phi_p(x)$ and $\phi_\sigma(x)$ are the twist-3 ones. For the Pion, up to twist 2 [48],

$$\phi_\pi(x) = 6x\bar{x}\{1 + a_1 C_2^{3/2}(\bar{x}-x) + a_2 C_4^{3/2}(\bar{x}-x)\}, \tag{A3}$$

with $a_1 = 0.44$, $a_2 = 0.25$, and the Gegenbauer polynomials are defined by

$$C_2^{3/2}(z) = \frac{3}{2}(5z^2-1), \qquad C_4^{3/2}(z) = \frac{15}{8}(21z^4 - 14z^2 + 1). \tag{A4}$$

Then, for the vector meson ρ, the corresponding matrix element of the hadronization projection operator is [47]

$$\bar{u}_{\alpha a}(xP')\Gamma(x,\ldots)_{\alpha\beta,ab,\ldots}v_{\beta b}(\bar{x}P') \to \frac{if_\rho}{4N_c}\int_0^1 dx M^\rho(x)_{\alpha\beta}\Gamma(x,\ldots)_{\alpha\beta,aa,\ldots}, \tag{A5}$$

$$M^\rho_{\alpha\beta} = M^\rho_{\alpha\beta\parallel} + M^\rho_{\alpha\beta\perp}, \tag{A6}$$

with

$$M^\rho_\parallel = -\frac{if_\rho}{4}\frac{m_\rho(\varepsilon^*\cdot n_+)}{2E}E\not{n}_-\phi_\parallel(u) - \frac{if_\perp m_\rho}{4}\frac{m_\rho(\varepsilon^*\cdot n_+)}{2E} \times\left\{-\frac{i}{2}\sigma_{\mu\nu}n_-^\mu n_+^\nu h_\parallel^{(t)}(u) - iE\int_0^u dv(\phi_\perp(v) - h_\parallel^{(t)}(v))\sigma_{\mu\nu}n_-^\mu\frac{\partial}{\partial k_{\perp\nu}} + \frac{h_\parallel'^{(s)}(u)}{2}\right\}\Big|_{k=up'} \tag{A7}$$

and

$$M^\rho_\perp = -\frac{if_\perp}{4}E\not{\varepsilon}^*_\perp\not{n}_-\phi_\perp(u) - \frac{if_\rho m_\rho}{4}\left\{\not{\varepsilon}^*_\perp g_\perp^{(v)}(u) - E\int_0^u dv(\phi_\parallel(v) - g_\perp^{(v)}(v))\not{n}_-\varepsilon^*_{\perp\mu}\frac{\partial}{\partial k_{\perp\mu}} + i\varepsilon_{\mu\nu\rho\sigma}\varepsilon_\perp^{*\nu}n_-^\rho\gamma^\mu\gamma_5 \times\left[n_+^\sigma\frac{g_\perp'^{(a)}(u)}{8} - E\frac{g_\perp^{(a)}(u)}{4}\frac{\partial}{\partial k_{\perp\sigma}}\right]\right\}\Big|_{k=up'}. \tag{A8}$$

Up to twist 2, the LCDA for a longitudinally polarized ρ meson is

$$\phi_{\rho,\parallel}(x) = 6x\bar{x}\{1 + a_1^\rho C_2^{3/2}(\bar{x}-x)\}; \tag{A9}$$

here $a_1^\rho = 0.18$.

In addition, the twist-2 LCDA for the K meson is [48]

$$\phi_K(x) = 6x\bar{x}\{1 + 0.51(\bar{x}-x) + 0.2C_2^{3/2}(\bar{x}-x)\}, \tag{A10}$$

and for a longitudinally polarized K^* meson, it is

$$\phi_{K^*,\parallel}(x) = 6x\bar{x}\{1 + 0.57(\bar{x}-x) + 0.07C_2^{3/2}(\bar{x}-x)\}. \tag{A11}$$

At last, using leading Fock states for heavy quarkonium, the quark's hadronizaiton projection operators are [27]

$$v(p_b)\bar{u}(p_c) \to \frac{1}{2\sqrt{2}}\gamma_5(P_{B_c} + m_b + m_c) \times\left(\frac{1}{\sqrt{\frac{m_b+m_c}{2}}}\psi_{B_c}(0)\right)\otimes\left(\frac{\mathbf{1}_c}{\sqrt{N_c}}\right),$$
$$v(p_{\bar{c}})\bar{u}(p_c) \to \frac{1}{2\sqrt{2}}\not{\varepsilon}(P_\Psi + m_c + m_c) \times\left(\frac{1}{\sqrt{\frac{m_c+m_c}{2}}}\psi_\Psi(0)\right)\otimes\left(\frac{\mathbf{1}_c}{\sqrt{N_c}}\right). \tag{A12}$$

The NLO Schrödinger wave function of J/ψ at the origin is determined by the leptonic decay width:

$$|\psi_{J/\psi}(0)|^2 = \frac{m_{J/\psi}^2}{16\pi\alpha^2 e_c^2}\frac{\Gamma(J/\psi\to e^+e^-)}{(1 + \pi\alpha_s C_F/v - 4\alpha_s C_F/\pi)}. \tag{A13}$$

APPENDIX B: RENORMALIZATION AND INFRARED SUBTRACTIONS

The renormalization constants include Z_2, Z_3, Z_m, and Z_g, corresponding to the heavy quark field, gluon field, quark mass, and strong coupling constant g, respectively. Here in our calculation, Z_g is defined in the modified minimal subtraction ($\overline{\rm MS}$) scheme, while for the other three, the on-shell (OS) scheme is adopted, which tells us the following:

$$\begin{aligned}
\delta Z_m^{\rm OS} &= -3C_F\frac{\alpha_s}{4\pi}\left[\frac{1}{\varepsilon_{UV}}-\gamma_E+\ln\frac{4\pi\mu^2}{m^2}+\frac{4}{3}+\mathcal{O}(\epsilon)\right],\\
\delta Z_2^{\rm OS} &= -C_F\frac{\alpha_s}{4\pi}\left[\frac{1}{\varepsilon_{UV}}+\frac{2}{\varepsilon_{IR}}-3\gamma_E+3\ln\frac{4\pi\mu^2}{m^2}+4+\mathcal{O}(\epsilon)\right],\\
\delta Z_3^{\rm OS} &= \frac{\alpha_s}{4\pi}\left[(\beta_0-2C_A)\left(\frac{1}{\varepsilon_{UV}}-\frac{1}{\varepsilon_{IR}}\right)+\mathcal{O}(\varepsilon)\right],\\
\delta Z_g^{\overline{MS}} &= -\frac{\beta_0}{2}\frac{\alpha_s}{4\pi}\left[\frac{1}{\varepsilon_{UV}}-\gamma_E+\ln 4\pi+\mathcal{O}(\varepsilon)\right],
\end{aligned}\tag{B1}$$

while for light quarks such as u and d quarks, the corresponding renormalization constant is

$$\delta Z_2^{\rm OS} = -C_F\frac{\alpha_s}{4\pi}\left(\frac{1}{\varepsilon_{UV}}-\frac{1}{\varepsilon_{IR}}\right).\tag{B2}$$

In the above, $\delta Z_i = Z_i - 1$, and $\beta_0 = (11/3)C_A - (4/3)T_f n_f$ is the one-loop coefficient of the QCD beta function; $C_A = 3$ and $T_F = 1/2$ attribute to the SU(3) group; μ is the renormalization scale.

We write the renormalized operator matrix elements as [28]

$$\langle Q_i\rangle_{\rm ren} = Z_\psi\hat{Z}_{ij}\langle Q_j\rangle_{\rm bare},\tag{B3}$$

where $i, j = 0, 8$, and $Z_\psi = Z_b^{1/2}Z_c^{1/2}Z_q$ contains the quark field renormalization factors of the massive b quark Z_b, the massive c quark Z_c, and the massless quarks Z_q, whereas $\hat{Z}$ is the operator renormalization matrix in the effective theory. It reads

$$\hat{Z} = 1 + \begin{pmatrix} 0 & 6 \\ \frac{4}{3} & -2 \end{pmatrix}\frac{\alpha_s}{4\pi}\frac{1}{\epsilon}.\tag{B4}$$

All of the soft IR divergences are canceled when summing them up, and Coulomb divergences can be canceled by the corresponding counterterm from the NLO Schrödinger wave function at the origin, while the left collinear divergences can be removed by the pion wave function's subtraction.

APPENDIX C: FORMULAS FOR THE NONFACTORIZABLE CONTRIBUTION

In this appendix, the asymptotic formulas for the one-loop nonfactorizable contribution are presented, where x is the collinear quark's momentum fraction in the pion and $z = m_c/m_b$ is the mass ratio for the charm quark and bottom quark. The results are valid in the heavy quark limit.

$$\begin{aligned}
T_{{\rm nf},0,x}^{(1)}(\eta_c) = \phi_\pi(x)\Bigg\{&\frac{2}{x}\ln\left(\frac{m_b^2}{\mu^2}\right)+\frac{2(x-1)\ln^2(x)}{3x(2x-1)}-\frac{2\left(\mathrm{Li}_2(\frac{x-1}{x})-\mathrm{Li}_2(\frac{x}{x-1})\right)}{3x}\\
&-\frac{1}{3(x-1)x(2x-1)}f_1-\frac{1}{3x(2x-1)}f_2+\frac{1}{3(2x-1)^3}f_3+\frac{1}{3(x-1)x(2x-1)^3}f_4\\
&+\frac{1}{3x^2(2x-1)^3}f_5+\frac{1}{3(x-1)x^2(2x-1)^3}f_6\Bigg\},
\end{aligned}\tag{C1}$$

$$T_{{\rm nf},0,x}^{(1)}(\Psi) = T_{{\rm nf},0,x}^{(1)}(\eta_c),\tag{C2}$$

with

$$f_1 = 2(x^2(\ln(2)-4)-x(2+2\ln(2))+2+\ln(2))\ln(x+1),$$

$$f_2 = 2(x-1)\left(-\mathrm{Li}_2\left(\frac{x+1}{2x^2}\right)+\mathrm{Li}_2\left(-\frac{1}{2x}\right)+2\mathrm{Li}_2\left(\frac{1}{x}\right)-\mathrm{Li}_2(-2x)+\mathrm{Li}_2(2(x+1))\right),$$

$$f_3 = 8(x-1)^2\left(\mathrm{Li}_2(4-2x)+2\mathrm{Li}_2\left(\frac{1}{1-x}\right)-\mathrm{Li}_2\left(-\frac{x-2}{2(x-1)^2}\right)+\mathrm{Li}_2\left(\frac{1}{2(x-1)}\right)-\mathrm{Li}_2(2x-2)\right),$$

$$f_4 = \ln(x)(-4(2x^2-3x+1)^2\,\ln(x+1) - 8x(x-1)^3\,\ln(2-x) + 3 + 6\,\ln(2) + x(2x(2x(-2x+2(5x-14)\ln(2)-3)+15+56\,\ln(2))-17-46\,\ln(2))),$$

$$f_5 = \ln(1-x)(x(x(4x(x-10x\,\ln(2)+5+18\,\ln(2))-37-38\,\ln(2))+19+4\,\ln(2)) + 2(x-1)x(\ln(x+1)+4(x-1)x(2\,\ln(2-x)+\ln(x+1)))-3),$$

$$f_6 = -8x^2(x-1)^3\ln^2(1-x) + (x-1)(x(x(x^2(20+8\,\ln(2))-x(72+16\,\ln(2)) + 79+8\,\ln(2))-32)+4)\ln(2-x) + x(2x(2x(28x^2-58x+45)-31) + \pi^2(x-1)^2 + x(103-2x(6x(6x-13)+83))\ln(2)+8-33\,\ln(2))+4\,\ln(2),$$

$$T^{(1)}_{8,nf,x}(\eta_c) = \phi_\pi(x)\Bigg\{\frac{-11C_A+48xN_c+2n_f-6}{9x}\,\ln\left(\frac{m_b^2}{\mu^2}\right) + \frac{9(x-1)\ln(z)-5x+2}{3(x-1)x}C_F - \frac{(3C_A-1)\ln^2(z)}{18x} - \frac{2(-3\,\ln(z)+5+3\,\ln(2))}{27x}n_f - \frac{\ln(z)}{54(x-1)x}((138x-144x\,\ln(2)-138+90\,\ln(2))C_A+144x + 96x^2\,\ln(1-x) - 96x^2\,\ln(x) - 96x\,\ln(1-x) + 96x\,\ln(x) + 372x\,\ln(2) - 144 - 210\,\ln(2)) + \frac{1}{N_c}\Bigg(\frac{2(\mathrm{Li}_2(\frac{x-1}{x})-\mathrm{Li}_2(\frac{x}{x-1}))}{3x} - \frac{(x-2)(x(10x-11)+2)\ln(1-\frac{x}{2})}{3(1-2x)^2x^2} + \frac{1}{3x(2x-1)}f_2 - \frac{1}{3(2x-1)^3}f_3 + \frac{1}{3(x-1)x(2x-1)^3}f_7 + \frac{1}{3x^2(2x-1)^3}f_8 + \frac{1}{3(x-1)x(2x-1)^3}f_9\Bigg) + C_A\Bigg(-\frac{(2x+1)(\mathrm{Li}_2(\frac{x-1}{x})-\mathrm{Li}_2(\frac{x}{x-1}))}{3x} - \frac{(x^2\mathrm{Li}_2(\frac{1-x}{2})-x^2\mathrm{Li}_2(\frac{x}{2})+2x\mathrm{Li}_2(\frac{x}{2})-\mathrm{Li}_2(\frac{1-x}{2}))}{(x-1)x} + \frac{1}{6x}f_2 - \frac{x-1}{3(2x-1)^3}f_3 + \frac{(-4x^2+x-1)\ln(x)\ln(2x+1)}{3x(2x-1)} - \frac{(x-2)(3x-2)(8x^2-6x+3)C_A\,\ln(1-\frac{x}{2})}{6(1-2x)^2(x-1)x} + \frac{\ln(x)}{6(x-1)x(2x-1)^3}f_{10} + \frac{\ln(1-x)}{6x^2(2x-1)^3}f_{11} - \frac{1}{6(x-1)x^2(2x-1)^3}f_{12} + \frac{1}{108(x-1)x^2(2x-1)^3}f_{13}\Bigg) - \frac{(x^2-x+2)(\mathrm{Li}_2(1-x)-\mathrm{Li}_2(1-\frac{x}{2}))}{9(x-1)x} + \frac{(x-3)(\mathrm{Li}_2(x)-\mathrm{Li}_2(\frac{x+1}{2}))}{9x} - \frac{3(x-2)\mathrm{Li}_2(\frac{x}{2})}{x-1} - \frac{7}{3}\left(\mathrm{Li}_2\left(\frac{x-1}{x}\right)-\mathrm{Li}_2\left(\frac{x}{x-1}\right)\right) + \frac{3(x+1)\mathrm{Li}_2(\frac{1-x}{2})}{x} + \frac{(x-2)(78x^2-51x-2)\ln(1-\frac{x}{2})}{18(x-1)x^2} + \frac{\ln(x)}{18(x-1)x}f_{14} + \frac{\ln(1-x)}{9(x-1)x^2}f_{15} + \frac{6}{108(x-1)x}f_{16}\Bigg\}, \tag{C3}$$

$$T^{(1)}_{8,nf,x}(\Psi) = T^{(1)}_{8,nf,x}(\eta_c) + \phi_\pi(x)\Bigg\{-\frac{16}{3}\,\ln\left(\frac{m_b^2}{\mu^2}\right) + \ln(z)\Bigg(\frac{16(x-1)x\,\ln(1-x)-16(x-1)x\,\ln(x)+36x\,\ln(2)-18\,\ln(2)}{9(x-1)x} - \frac{2(2x-1)\ln(2)C_A}{3(x-1)x}\Bigg) + \frac{C_A}{18(x-1)x}f_{17} + \frac{1}{18(x-1)x}f_{18}\Bigg\}, \tag{C4}$$

with

$$f_7 = \ln(x)(4(2x^2-3x+1)^2\,\ln(x+1) + (x+3)(2x-1)^3 + 8x(x-1)^3\,\ln(2-x) - 2(4x(x(5x-9)+5)-3)(x-1)\ln(2)),$$

$$f_8 = \ln(1-x)(x(x(-4x(x+5)+8x(5x-9)\ln(2)+37+38\,\ln(2))-19-4\,\ln(2)) + 2(x-1)x(-\ln(x+1)-4(x-1)x(2\,\ln(2-x)+\ln(x+1)))+3),$$

$$f_9 = 24x^3\ \ln(2)\ln(4-2x) - 8x(x^3+3x-1)\ln(2)\ln(2-x) + x(4x^3(13\ \ln(2)-28) - 8x^2(-29+3\ln^2(2)+8\ \ln(2)) + 15x(\ln(2)-12) + 62 + 8\ \ln(2)) - \pi^2(x-1)^2 + 8x(x-1)^3\ln^2(1-x) + 2x(x(-4(x-3)x-13)+6)\ln^2(x) - 2\ln^2(x) + 4i\pi(x-1)^2\ \ln(2) + (2x(x(x(x(4\ \ln(2)-16)+8-12\ \ln(2))+12+13\ \ln(2)) - 2(5+3\ \ln(2)))+2\ \ln(2))\ln(x+1) + 4\ \ln(x+1) - 8 - 3\ \ln(2),$$

$$f_{10} = (16x(x-1)^4\ \ln(2-x) + 4(2x-1)^3(x-1)^2\ \ln(x+1) - 2x(x-1)(2x(2x(4x-8-7\ \ln(2))+10+17\ \ln(2)) - 3(2+5\ \ln(2))) + 2(1-2x)^2(x(4x-1)+1)(x-1)\ln(2x+1) + 1 + 2\ \ln(2)),$$

$$f_{11} = (-32x^2(x-1)^3\ \ln(2-x) - 2x(2x-1)^3(x-1)\ln(x+1) + x(x(4x(x(20x-37-20\ \ln(2)) + 29 + 30\ \ln(2)) - 51 - 52\ \ln(2)) + 12 + \ln(16)) - 1),$$

$$f_{12} = \left(-(x-2)x(2x-1)(3x-2)(8x^2-6x+3)\ln\left(1-\frac{x}{2}\right) + \ln(1-x)(-32x^6\ \ln(4-2x) + 32(2x(x(2x-3)+2)-1)x^2\ \ln(2-x) + x(x(x(4x(x(4x(5+2\ \ln(2))-57 - 20\ \ln(2))+66+50\ \ln(2))-167-172\ \ln(2))+7(9+8\ \ln(2)))-13-4\ \ln(2)) - 2(x-1)^2(2x-1)^3x\ \ln(x+1)+1) - 2(x-1)x(x(4x-1)+1)(1-2x)^2\ \ln(x)\ln(2x+1)\right),$$

$$f_{13} = (x(6(x(x(72x^2-62x-23)+41)-13)(2x-1)\ln(2) + 8(47x-20)(2x-1)^3 - 3\pi^2(x(8x(x(20x-47)+39) - 101)+8) + 36(x(2x(2x(2x(x+3)-17)+29)-23)+4)\ln^2(2)) + 18(16x^2(x-1)^4\ln^2(1-x) + x((1-2x)^2((2x-1)\left(-6(x^2-1)\ln^2\left(\frac{x+1}{2}\right) + (-2(x-2)x-3)\ln^2(x) + 2(x-1)^2\ \ln(2)\ln(x+1)\right) + 2(x((5-4x)x-2)+1)\ln(x)\ln(2x+1)\right) - (x-2)(3x-2)(8x^2-6x+3)(2x-1)\ln\left(1-\frac{x}{2}\right) + 6(x-2)x\left(2x-1)^3\ln^2\left(1-\frac{x}{2}\right)\right) + (x-1)\ln(1-x)(-32x^2(x-1)^3\ \ln(2-x) - 2x(2x-1)^3(x-1)\ln(x+1) + x(x(4x(x(20x-37-20\ \ln(2))+29+30\ \ln(2))-51 - 52\ \ln(2))+12+4\ \ln(2))-1)) - 288x^2(x-1)^4\ \ln(2)\ln(4-2x)),$$

$$f_{14} = (x(180x - 58x\ \ln(2) - 139 + 40\ \ln(2)) - 2((x-1)x+2)\ln(1-x) + 2((x-1)x+2)\ln(2-x) + 64(x-1)x\ \ln(2x) - 2 - 4\ \ln(2)),$$

$$f_{15} = (x(x^2\ \ln(128x) - 32(x-1)x\ \ln(2-2x) + (3-4x)\ln(2x) - (x-3)(x-1)\ln(x+1)) + x(x(x(15+22\ \ln(2))-9-28\ \ln(2))-9)+3),$$

$$f_{16} = (13\ \ln(2)(\ln(32)-6x^2) + x(384x-380+(19-117\ \ln(2))\ln(2))+20-30\ \ln(2)) + 5\pi^2(12x-7) + 6\ln^2(x) - 324\ln^2\left(\frac{x+1}{2}\right) + 6\left(64(x-1)x\ln^2(1-x) + 2x\left(-27(x-2)\ln^2\left(1-\frac{x}{2}\right) + 4(9-8x)\ln^2(x) + 27x\ln^2\left(\frac{x+1}{2}\right)\right) - 2((x-1)x+2)\ln(2)\ln(2-x) + (2x((x-4)\ln(2)+16) + 6\ \ln(2))\ln(x+1)\right) + 192\ \ln(x+1),$$

$$f_{17} = (-6(x-1)x\ln^2(1-x) + 6(x-1)x\ln^2(x) + 2(2x-1)(\pi^2 - 3\ln^2(2)) + 24(x-1)x\ \ln(2)\ln(1-x) - 24(x-1)x\ \ln(2)\ln(x)),$$

$$f_{18} = 32(x-1)x\mathrm{Li}_2\left(\frac{x-1}{x}\right) - 32(x-1)x\mathrm{Li}_2\left(\frac{x}{x-1}\right) - 192x^2 - 46x^2\ln^2(1-x) + 46x^2\ln^2(x) + 64x^2\ \ln(2-2x)\ln(1-x) - 72x^2\ \ln(2)\ln(1-x) - 48x^2\ \ln(1-x) + 72x^2\ \ln(2)\ln(x) - 48x^2\ \ln(x) - 64x^2\ \ln(x)\ln(2x) - 10\pi^2 x + 160x + 46x\ln^2(1-x) - 46x\ln^2(x) + 28x\ln^2(2) - 64x\ \ln(2-2x)\ln(1-x) + 72x\ \ln(2)\ln(1-x) + 64x\ \ln(1-x) - 72x\ \ln(2)\ln(x) + 16x\ \ln(x) + 64x\ \ln(x)\ln(2x) + 8x\ \ln(2)\ln(2) - 44x\ \ln(2) - 16\ \ln(1-x) + 4\pi^2 - 18\ln^2(2) + 12\ \ln(2) + 32\ \ln(2).$$

[1] N. Brambilla *et al.* (Quarkonium Working Group), Report No. CERN-2005-005.
[2] F. Abe *et al.* (CDF Collaboration), Phys. Rev. Lett. **81**, 2432 (1998).
[3] A. Abulencia *et al.* (CDF Collaboration), Phys. Rev. Lett. **97**, 012002 (2006).
[4] V. M. Abazov *et al.* (D0 Collaboration), Phys. Rev. Lett. **102**, 092001 (2009).
[5] T. Aaltonen *et al.* (CDF Collaboration), Phys. Rev. Lett. **100**, 182002 (2008).
[6] V. M. Abazov *et al.* (D0 Collaboration), Phys. Rev. Lett. **101**, 012001 (2008).
[7] R. Aaij *et al.* (LHCb Collaboration), Phys. Rev. Lett. **109**, 232001 (2012).
[8] R. Aaij *et al.* (LHCb Collaboration), Phys. Rev. Lett. **108**, 251802 (2012).
[9] R. Aaij *et al.* (LHCb Collaboration), J. High Energy Phys. 09 (**2013**) 075.
[10] R. Aaij *et al.* (LHCb Collaboration), Phys. Rev. D **87**, 071103 (2013).
[11] R. Aaij *et al.* (LHCb Collaboration), Phys. Rev. D **87**, 112012 (2013).
[12] C.-H. Chang, C. Driouichi, P. Eerola, and X.-G. Wu, Comput. Phys. Commun. **159**, 192 (2004).
[13] C.-H. Chang and X.-G. Wu, Eur. Phys. J. C **38**, 267 (2004).
[14] Y.-N. Gao, J.-B. He, P. Robbe, M.-H. Schune, and Z.-W. Yang, Chin. Phys. Lett. **27**, 061302 (2010).
[15] A. Deandrea, N. Di Bartolomeo, R. Gatto, and G. Nardulli, Phys. Lett. B **318**, 549 (1993).
[16] H.-n. Li and H.-L. Yu, Phys. Rev. D **53**, 2480 (1996).
[17] M. Beneke, G. Buchalla, M. Neubert, and C. T. Sachrajda, Phys. Rev. Lett. **83**, 1914 (1999).
[18] M. Beneke, G. Buchalla, M. Neubert, and C. T. Sachrajda, Nucl. Phys. **B591**, 313 (2000).
[19] M. Beneke and S. Jager, Nucl. Phys. **B751**, 160 (2006); , Nucl. Phys. **B736**, 34 (2006); , J. High Energy Phys. 05 (**2007**) 019.
[20] H.-Y. Cheng and S. Oh, J. High Energy Phys. 09 (**2011**) 024; G. Zhu, J. High Energy Phys. 05 (**2010**) 063.
[21] G. T. Bodwin, E. Braaten, and G. P. Lepage, Phys. Rev. D **51**, 1125 (1995); Phys. Rev. D **55**, 5853(E) (1997).
[22] G. Buchalla, A. J. Buras, and M. E. Lautenbacher, Rev. Mod. Phys., **68**, 1125 (1996).
[23] T. Hahn, Comput. Phys. Commun. **140**, 418 (2001).
[24] R. Mertig, M. Böhm, and A. Denner, Comput. Phys. Commun., **64**, 345 (1991).
[25] T. Hahn and M. Perez-Victoria, Comput. Phys. Commun., **118**, 153 (1999).
[26] J. G. Körner, D. Kreimer, and K. Schilcher, Z. Phys. C **54**, 503 (1992).
[27] C.-F. Qiao, L.-P. Sun, and R.-L. Zhu, J. High Energy Phys. 08 (**2011**) 131; L.-B. Chen, C.-F. Qiao, and R.-L. Zhu, Phys. Lett. B **726**, 306 (2013).
[28] G. Bell, Ph.D. thesis, Ludwig Maximilian University of Munich, 2006, arXiv:0705.3133.
[29] C.-F. Qiao, P. Sun, and F. Yuan, J. High Energy Phys. 08 (**2012**) 087.
[30] C.-F. Qiao and R.-L. Zhu, Phys. Rev. D **87**, 014009 (2013).
[31] R. K. Ellis and G. Zanderighi, J. High Energy Phys. 02 (**2008**) 002.
[32] S. Dittmaier, Nucl. Phys. **B675**, 447 (2003).
[33] K. Nakamura *et al.* (Particle Data Group), J. Phys. G **37**, 075021 (2010).
[34] E. J. Eichten and C. Quigg, Phys. Rev. D **49**, 5845 (1994).
[35] V. V. Kiselev, A. E. Kovalsky, and A. K. Likhoded, Nucl. Phys. **B585**, 353 (2000).
[36] V. V. Kiselev, arXiv:hep-ph/0211021.
[37] C. H. Chang and Y. Q. Chen, Phys. Rev. D **49**, 3399 (1994).
[38] A. Abd El-Hady, J. H. Munoz, and J. P. Vary, Phys. Rev. D **62**, 014019 (2000).
[39] M. A. Ivanov, J. G. Körner, P. Santorelli, Phys. Rev. D **73**, 054024 (2006).
[40] J. Sun, D. Du, and Y. Yang, Eur. Phys. J. C **60**, 107 (2009).
[41] A. Y. Anisimov, P. Y. Kulikov, I. M. Narodetsky, and K. A. Ter-Martirosian, Phys. At. Nucl. **62**, 1739 (1999).
[42] P. Colangelo and F. De Fazio, Phys. Rev. D **61**, 034012 (2000).
[43] D. Ebert, R. N. Faustov, and V. O. Galkin, Phys. Rev. D **68**, 094020 (2003).
[44] B. Aubert *et al.* (*BABAR* Collaboration) Phys. Rev. Lett. **99**, 261801 (2007).

[45] K. C. Yang, Nucl. Phys. **B776**, 187 (2007).
[46] A. K. Likhoded and A. V. Luchinsky, Phys. Rev. D **81**, 014015 (2010); A. V. Luchinsky, Phys. Rev. D **86**, 074024 (2012).
[47] M. Beneke, Th. Feldmann, Nucl. Phys. **B592**, 3 (2000).
[48] P. Ball, V. M. Braun, Y. Koike and K. Tanaka, Nucl. Phys. **B529**, 323 (1998); C.-D. Lü and M.-Z. Yang, Eur. Phys. J. C **28**, 515 (2003).
[49] G. Bell and T. Feldmann, J. High Energy Phys. 04 (**2008**) 061.